Self-Ordering of Buckling, Bending, and Bumping Beams

Arman Guerra, Anja C. Slim, Douglas P. Holmes, and Ousmane Kodio

Phys. Rev. Lett. **130**, 148201 — Published 3 April 2023

DOI: 10.1103/PhysRevLett.130.148201

Self-Ordering of Buckling, Bending, and Bumping Beams

Arman Guerra,[1] Anja Slim,[2,3] Douglas P. Holmes,[1] and Ousmane Kodio[4,*]

[1]*Department of Mechanical Engineering, Boston University, Boston, Massachusetts 02215, USA*
[2]*School of Mathematics, Monash University, Victoria 3800, Australia*
[3]*School of Earth, Atmosphere and Environment, Monash University, Victoria 3800, Australia*
[4]*Department of Mathematics, Massachusetts Institute of Technology, Cambridge, Massachusetts 02139, USA*

(Dated: January 17, 2023)

A collection of thin structures buckle, bend, and bump into each other when confined. This contact can lead to the formation of patterns: hair will self-organize in curls; DNA strands will layer into cell nuclei; paper, when crumpled, will fold in on itself, forming a maze of interleaved sheets. This pattern formation changes how densely the structures can pack, as well as the mechanical properties of the system. How and when these patterns form, as well as the force required to pack these structures is not currently understood. Here we study the emergence of order in a canonical example of packing in slender structures, *i.e.* a system of parallel confined elastic beams. Using tabletop experiments, simulations, and standard theory from statistical mechanics, we predict the amount of confinement (growth or compression) of the beams that will guarantee a global system order, which depends only on the initial geometry of the system. Furthermore, we find that the compressive stiffness and stored bending energy of this meta-material are directly proportional to the number of beams that are geometrically frustrated at any given point. We expect these results to elucidate the mechanisms leading to pattern formation in these kinds of systems, and to provide a new mechanical meta-material, with a tunable resistance to compressive force.

When thin structures pack, there is a competition between elasticity, which often encourages pattern formation and densification, and geometric constraints. For example, paper, when crumpled into a ball, forms complex three-dimensional swirls [1, 2], and DNA strands inserted into cell nuclei fold and pack into layers [3, 4]. In some cases, these densification processes are resisted by friction [5, 6] and geometrical incompatibilities in the deformation of the materials [7–10]. The formation of patterns has been studied thoroughly in cases where thin structures are adhered to a substrate [11–14], sheets are constrained in a ring [6, 15, 16], and rods are inserted into a container [17–19]. However, the question of to what degree the rods and sheets will order themselves in these complex and random packing processes is still open.

In structured arrangements of elastic beams, the competition between order and geometric frustration has been used to great effect in the design of materials with novel and programmed properties [20–23]. There are many models in statistical mechanics to rationalize the emergence of order [24, 25], and in some cases these models have been extended to study frustration, fluctuation, and shape-change in thin elastic structures [26–29]. However, these models are insufficient to capture the ordering of beams because of the difficulty of finding and modeling the interaction forces between adjacent elements. For example, consider a simple 1-D version of the ordering of packed beams, the gills of a mushroom (see Figure 1a). If the mushroom dries and shrinks, the gills will at first buckle, and then bump into each other. Reminiscent of the 1-D Ising model for magnetism [24], the ground state of this system occurs when all gills point in the same direction (shown in an analogous experiment in Figure 1b, right). However, here there exists a hierarchy of disordered meta-stable states in the shallow-post-buckling regime, where the gills self-organize into "clumps," and leave "holes" where they have separated (Figure 1a, middle).

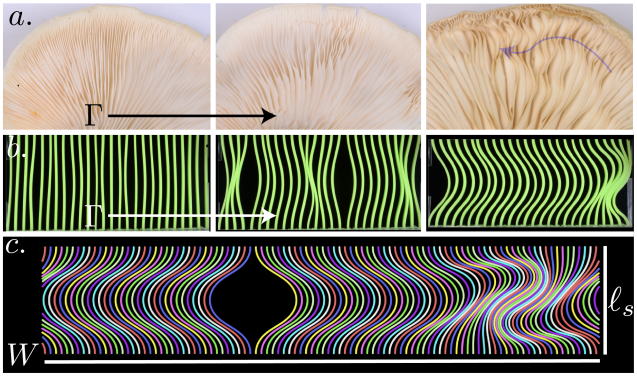

FIG. 1: (a) An oyster mushroom that has been left in the open air to dry (approximately one day between consecutive pictures). During this drying process, the gills become compressed along their length, causing them to buckle (middle) and then align (right). (b) Experimental observations of a similar phenomenon in a system of slender parallel plates compressed in an Instron. (c) A numerical experiment of the same system. Videos of a typical experiment (SI video 1) and simulation (SI video 2) are available.

In this Letter, we consider a simplified version of this system: an array of N parallel elastic beams confined to a vertical space ℓ_s that is shorter than their length ℓ, and equally spaced inside of a box of width W, such that the distance between the centers of any two adjacent beams is $d = W/N$ (Figure 1c). We characterize the control parameter of the system to be the confinement factor $\Gamma = \ell/\ell_s$. If the beams are initially perturbed in random directions, we observe behavior reminiscent

of a phase transition, where the initial disordered state (beams buckled in random directions) will gradually decay to the fully-ordered ground state (all beams aligned in one direction) as Γ increases. We therefore ask the following two questions: First, when and how much will the beams align; can we predict how order will emerge? Second, how does the mechanical response of the system depend on the degree of order and its emergent topology; conversely could we use this emergent topology in the design of tunable-stiffness materials?

To investigate this state transition experimentally, we built a stiff acrylic two-piece mount that served to clamp many slender elastic plates at two of their opposite edges (effecting clamped-clamped boundary conditions). We inserted sheets of PVS (thickness $h = 1.5$ mm, number $N = 26$) into the mounts, and compressed the system uniformly with an Instron, which allowed us to measure Γ, as well as the force response of the arrangement of beams (Figure 1b). We then performed an ensemble of non-thermal quenches on this array of beams – that is, we iso-statically compressed the beams many times, manually biasing each beam by hand to initially buckle to the right or left based on a random coin-flip at the start of each experiment (further details in SI section 1). Just as we see in the case of the mushroom (Figure 1a), any adjacent beams buckling towards each other will eventually make contact and form clumps (Figure 1b, middle). After enough confinement, these clumps become unstable and decompose, and the beams eventually all point in one direction (Figure 1b, right).

We parametrize the direction of the buckling of each beam using what we call the "tropism" where $T_i = 0$ when beam i is un-buckled, and $T_i = +1$ (-1) if it is buckled to the right (left), as shown in Figure 2a. To account for beams that are no longer in the first buckling mode because of contact with other adjacent beams or with the walls, we consider that a beam is buckled to the right (left) if the portion of the beam halfway up the box is farther to the right (left) than its ends. We can average the behavior of all beams into an overall system tropism

$$\bar{T} = \left| \frac{1}{N} \sum_{i=1}^{N} T_i \right|. \qquad (1)$$

Note that $\bar{T} \approx 0$ when the beams are randomly directed, and $\bar{T} \approx 1$ when the beams are all aligned (Figure 1b, right). We plot the ensemble-average of $\bar{T}$ at increasing Γ for a fixed beam spacing, number, thickness, and initial length in Figure 2b (♦), and indeed find a gradual increase in the average order of the system. We find large variance in $\bar{T}$ (*i.e.* large error bars) for different random initializations of the beam buckling directions. This large variance results from the fact that order arises at different Γ for different random initializations of the

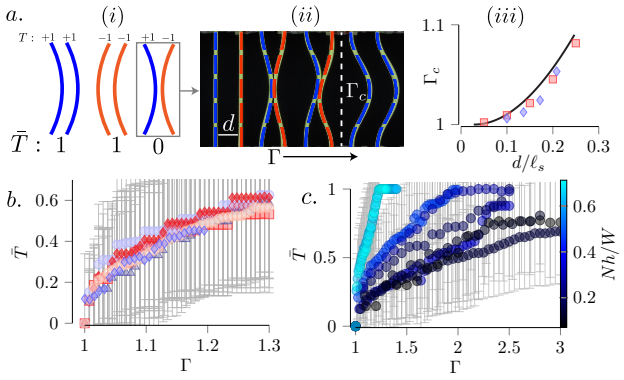

FIG. 2: The emergence of order for (a) two beams and (b & c) many beams. (a *i.*) Illustrated examples of T_i (+1, blue; −1, orange) (a *ii.*) Experiments (green) overlaid with simulations (blue and orange) of two beams that buckle towards each other. There are two meta-stable "clumped" $\bar{T} = 0$ states (vertically and rotationally symmetric) however when $\Gamma > \Gamma_c$, $\bar{T} = 1$. (a *iii.*) Γ_c increases with the normalized distance between two beams d/ℓ_s (experiments – ♦, simulations – ■, model – black line, SI section 2) (b) $\bar{T}$ for experiments and simulations of many beams ($N = 26$, $W = 140$ mm, $\ell_s = 54$ mm, $h = 1.54$ mm, average $d = 5.4$ mm, number of ensemble measurements: experiment – 25, simulation – 100) (c) $\bar{T}$ increases with Γ with a rate highly dependent on N, d, W, h, and ℓ_s.

beams. We can compare this with the behavior of two beams buckling towards each other (Figure 2a *ii* and *iii*) and find that for the many-beam case, the clumps remain stable (and therefore $\bar{T} < 1$) at much higher Γ for the same normalized beam spacing d/ℓ_s (Figure 1c).

To eliminate any imperfections in the experimental set-up and other forces such as gravity, we replicated the geometry of our physical experiments using numerical experiments (ensemble $\bar{T}$ shown in Figure 2b, ▲) in the Large-scale Atomic/Molecular Massively Parallel Simulator (LAMMPS [30], visualizations in Ovito [31]) adopting a similar protocol as [32] to simulate the mechanics of the elastic beams (SI section 3). We also include simulations with varying coefficient of sliding friction ($\mu_s = 0$, frictionless, ■; $\mu_s = 1$, rubber-like, ♦; $\mu_s = 2$, highly frictional, ♦), and different beam-end (pin-pin, ●), and vertical box edge (periodic, ■) boundary conditions. Additionally, we performed simulations where the distances between the beams was uniformly randomly distributed with a lower bound of $1.2h$ and an upper bound such that the average distance between the beams is the same as the model experiment (SI video 3, ●). We find good agreement between experiments and simulations, and furthermore the tropism $\bar{T}$ is statistically independent of the degree of friction, boundary conditions, and beam spacing variability. The lack of dependence on friction is somewhat unique when compared to other work on the packing of slender structures [5, 6, 15–19]. However, our set-up is designed specifically to study the emergence of order, not the packing of the elastic structures in space.

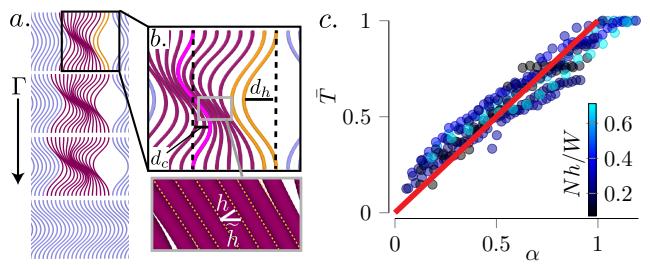

FIG. 3: Understanding beam alignment. (a) A step-by-step illustration of clump-hole annihilation, with simulations at increasing Γ from top to bottom. Clumped beams are colored purple, and all others are colored by their tropism ($T_i = 1 \rightarrow$ blue, $T_i = -1 \rightarrow$ orange). (b) Illustration of the parameters in our mathematical model. (c) The ensemble value of $\bar{T}$ as a function of α (prediction from Equation 2, red). Error bars are the same as in Figure 2c, left off for clarity.

In our system, order arises at relatively low confinement compared to other studies, and since understanding this ordering is our aim, we do not consider a highly-packed regime, where the beams would begin to slide against each other and the walls, and friction would play a larger role. We discuss this further in section 4 of the SI. Hence, without loss of generality, we performed simulations of clamped-clamped, evenly spaced beams without friction in a periodic box, with the expectation that the results apply broadly. We varied the beam density as well as the number of beams, plot $\bar{T}$ as a function of Γ in Figure 2c, and find that $\bar{T}$ strongly depends on the geometric parameters of the box.

In Figure 3a we show a series of simulations with increasing Γ. We find that beams align when clumps and holes "meet" and annihilate, that is, the space between the center of a clump and a hole is completely taken up by the horizontal deflection of the hole (d_h) and the clump (d_c), as well as the sum of the thicknesses of the beams between them (Figure 3b, more detail in SI section 5). We can use this mechanism to predict $\bar{T}$ as a function of Γ. We would expect that $\bar{T} = 1$ when the final clump meets and annihilates with the final hole. For simplicity we will consider the case where the edges of the box are periodic, and as such the maximum possible distance between the final clump-hole pair is $W/2$. If we approximate the shape of a beam as a triangle, using the Pythagorean theorem, $d_h \approx \frac{1}{2}\ell_s\sqrt{\Gamma^2 - 1}$. We can further approximate the center beam of a clump as a mode-2 buckled elastica, and so $d_c \approx d_h/2$.

In experiments and simulations, we observe that clumps and holes do not move laterally as the beams are confined, and therefore, before annihilation, the number of beams between a clump and a hole N_b stays the same. However, the effective horizontal thickness $\widetilde{h}$ of the beams changes, as shown in Figure 3b. If we keep our triangular approximation for the shape of the beams, we get that $\widetilde{h} \approx h\Gamma$ and therefore the additional space that each beam takes up is $\widetilde{h} - h = h(\Gamma - 1)$.

When the maximum amount of initially empty space between a clump and a hole ($W/2 - Nh/2$) is taken up by these three previously mentioned lengths ($d_h + d_c + N_b h(\Gamma - 1)$), all clumps and holes will have met and annihilated, and $\bar{T} \rightarrow 1$. In the case where the last clump and hole are as far apart as they can be, $N_b = N/2$, so the fraction of the horizontal space between the clump and hole taken up by the beams, which we will call the "porosity" α, is $\alpha = [d_h + d_c + N(\widetilde{h} - h)/2]/(W/2 - Nh/2)$. In Figure 3c, we plot $\bar{T}$ against α and find that, as we expect, for all geometries, $\bar{T} \approx 1$ when $\alpha = 1$. More than that, however, it seems that the tropism is *approximately equal* to α, or in other words, rearranging and inserting our previously derived values for the clump and hole deflections,

$$\bar{T} \approx \alpha = \frac{\frac{1}{2}(\Gamma - 1)hN + \frac{3}{4}\ell_s\sqrt{\Gamma^2 - 1}}{W/2 - Nh/2}. \qquad (2)$$

This comes from the fact that as the beams are confined, the number of clumps and holes which make contact and annihilate is proportional to the space that the beams take up. We note that, as can be seen from Figure 3c, even when $\alpha = 1$, there are some cases where $\bar{T}$ is slightly less than 1. We expect that these small discrepancies come from the fact that, rather than explicitly deriving d_h, d_c, and $\widetilde{h}$, we have approximated their values. A more thorough theoretical treatment of the beams might improve the quality of our prediction, however, we believe that these approximations are sufficiently elucidating for the purposes of this work.

Now that we understand when the beams will become ordered, we turn to our second question: how do the beams respond to the imposed compression when they are not ordered? This is analogous to why it requires less force to confine paper to a target volume through folding than through crumpling [2]: a larger degree of geometrical frustration in thin structures often leads to more stored energy [33]. We can observe this directly in our system. In Figure 4 we plot the normalized compressive force $\widetilde{F}_i = F_i/F_1$ of each beam in a clamped-clamped, periodic, frictionless simulation, where F_i is the compressive force applied to beam i, and F_1 is the compressive force applied to a single beam with the same boundary conditions, compressed to the same Γ and no neighboring beams. We simultaneously define and plot the normalized bending energy $\widetilde{U}_{bi} = U_{bi}/U_{b1}$ in the same way, where U_{bi} is the bending energy of beam i, and U_{b1} is the corresponding bending energy of the beam from which we derive F_1. We superimpose these plots onto the simulated configurations. For beams that are not in clumps, and therefore have no contacts, $\widetilde{F}_i = \widetilde{U}_{bi} = 1$. In contrast, beams that are in contact with other beams in a clump and are geometrically frustrated [33] have a higher $\widetilde{F}_i$ and $\widetilde{U}_{bi}$, as they cannot find their lowest-energy

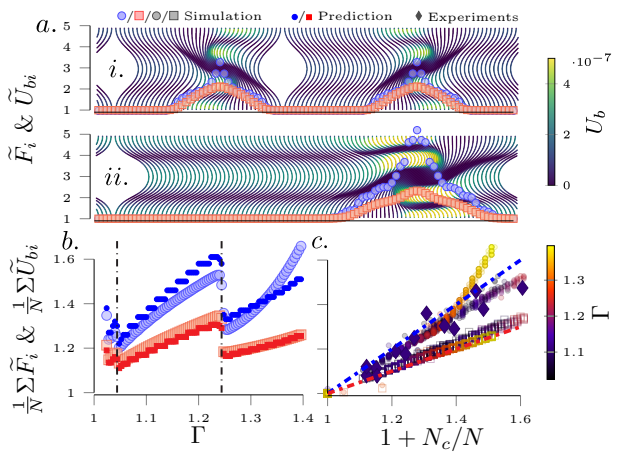

FIG. 4: Ordering affects compressive stiffness. (a) Snapshots of a simulation at $\Gamma = 1.18$ (i) and $\Gamma = 1.38$ (ii), superimposed with the vertical compressive force (F_i, ●) and bending energy (U_{bi}, ■) of each beam normalized by the force and bending energy of a beam which is not part of a clump (F_1, U_{b1}). (b) The total compressive force (●) and bending energy (■) of the same system of beams as a function of Γ, normalized by the compressive force and bending energy of the system if all the beams were buckled in the same direction. Predictions from our approximated model (Equation 3) are ● (F) and ■ (U_b). Vertical lines show places where a clump and hole annihilate (SI video 4) (c) Normalized force and bending energy against $1 + N_t/N$ together with our predictions from Equation 3 (simulation U_b – squares, predicted U_b – red line, simulation F – circles, experiment F – diamonds, predicted F – blue line). Gray in the legend indicates coloration by Γ.

state. These results indicate that our system is behaving like a mechanical meta-material, an object that gets its properties not only from the material that it is made of, but also its internal geometry [23].

Previously, we noted that the beam at the center of a clump has the approximate shape of a mode-2 elastica. We would expect that $U_b \propto n$ where n is the mode number of the beam (since doubling n doubles the average curvature in the beam), so for the central beam in the clump we expect that $\widetilde{U}_{bi} \approx 2$. This is confirmed in Figure 4a, even for very large Γ. To estimate F_i for the central beam of a clump, we performed additional simulations of a single beam, where the slope at the vertical center of the beam was forced to match the slope derived from our triangular approximation of the beam shape. In these simulations we found that $\widetilde{F}_i \approx 3$. In Figure 4a, we find that the maximum value of $\widetilde{F}_i$ is indeed approximately 3 for most of the simulation, but increases for very large Γ, which we expect comes from a deviation of the true beam shape from our approximation.

In Figure 4a we see that $\widetilde{F}_i$ and $\widetilde{U}_{bi}$ for the beams in the clump seems to increase linearly from ≈ 1 at the edge of the clump, to the maximum value at the clump center. If we use our earlier approximations for these maximum values ($\widetilde{U}_{bi} \approx 2$ and $\widetilde{F}_i \approx 3$), we might expect that, on average, a beam in a clump has $\widetilde{U}_{bi} \approx 1.5$ and $\widetilde{F}_i \approx 2$. Hence, we would expect that the total force and bending energy in our arrangement of beams is

$$\begin{aligned} F &= F_1(N + N_c), \\ U_b &= U_{b1}(N + N_c/2), \end{aligned} \tag{3}$$

where N_c is the number of beams that are in a clump. In Figure 4b, we plot the total normalized force $F/(NF_1)$ (●) and bending energy $U_b/(NU_{b1})$ (■) of the specific simulation run pictured in Figure 4a, along with their estimated values from the number of clumped beams as given by Equation 3 and find good agreement, except at high Γ, when the normalized force estimate starts to fail as we expected. In Figure 4c, we plot $F/(NF_1)$ (circles) and $U_b/(NU_{b1})$ (squares) against $1+N_c/N$ and find that for a wide variety of box geometries, $U_b/(NU_{b1})$ collapses to $(1 + N_c/N)/2$ for all data, and $F/(NF_1)$ collapses approximately to $1 + N_c/N$ for all data except for that at very high Γ, both of which reinforce the appropriateness of Equation 3. We expect that this error in the prediction of $F/(NF_1)$ could be reduced with an analytical treatment of $\widetilde{F}_i$ for the beam at the center of a clump (which may itself depend on Γ), which could replace the value of 3 that we approximated from the model simulation mentioned above.

In this work we have studied how many parallel beams clamped at their ends and confined in a box order themselves, and found that at high enough Γ, $\bar{T} \to 1$. We also found that the compressive stiffness of the metamaterial made up of these buckling beams is proportional to the number of beams in a clump, potentially allowing the stiffness to be manually or automatically tuned. We expect that changes in the geometry that we have studied could lead to a large dependence on friction, as is the case in many other systems of slender contacting structures [5, 34–38], creating an additional route for novel functionalities. Furthermore, any intrinsic thermal motion [29], adhesion [39, 40], curvature, or any transverse loading or long-range potentials may affect the ordering and mechanical properties of the system, potentially providing deeper analogies to other work in statistical mechanics [25, 26], and more tunability. So far, we have only considered beams with two motion-restricted ends and fixed or periodic box edges; further studies could consider cases where one end of the beams is free (like hair, microtubules [41], or a carbon nanotube forest [42, 43]) or restricted only by friction with a wall, or where a lateral edge is clamped, such as in the case of the mushroom gills. We also note that, as the beams are compressed, a transverse force (the compression) turns into a longitudinal transfer, namely the redirection of the beams. This could provide a method to redirect and control mechanical waves [44, 45].

ACKNOWLEDGEMENTS

We thank Abigail Plummer, Harold Park, and Dominic Vella for helpful discussion. We also gratefully acknowledge the financial support from DARPA (#HR00111810004) and from NSF CMMI–CAREER through Mechanics of Materials and Structures (#1454153), and the computing resources of the Boston University Shared Computing Cluster.

* kodio@mit.edu

[1] A. D. Cambou and N. Menon, Proceedings of the National Academy of Sciences **108**, 14741 (2011).

[2] S. Deboeuf, E. Katzav, A. Boudaoud, D. Bonn, and M. Adda-Bedia, Physical Review Letters **110**, 104301 (2013).

[3] D. E. Smith, S. J. Tans, S. B. Smith, S. Grimes, D. L. Anderson, and C. Bustamante, Nature **413**, 748 (2001).

[4] J. Kindt, S. Tzlil, A. Ben-Shaul, and W. M. Gelbart, Proceedings of the National Academy of Sciences **98**, 13671 (2001).

[5] H. Alarcón, T. Salez, C. Poulard, J.-F. Bloch, É. Raphaël, K. Dalnoki-Veress, and F. Restagno, Physical Review Letters **116**, 015502 (2016).

[6] S. Alben, Proceedings of the Royal Society A **478**, 20210742 (2022).

[7] J. Andrejevic, L. M. Lee, S. M. Rubinstein, and C. H. Rycroft, Nature Communications **12**, 1 (2021).

[8] G. Domokos, P. Holmes, and B. Royce, in *Mechanics: From Theory to Computation* (Springer, 2000), pp. 413–446.

[9] B. Roman and A. Pocheau, EPL (Europhysics Letters) **46**, 602 (1999).

[10] A. Pocheau and B. Roman, Physica D: Nonlinear Phenomena **192**, 161 (2004).

[11] M. A. Biot, *Bending of an infinite beam on an elastic foundation* (American Society of Mechanical Engineers, 1937).

[12] D. A. Dillard, B. Mukherjee, P. Karnal, R. C. Batra, and J. Frechette, Soft Matter **14**, 3669 (2018).

[13] O. Kodio, I. M. Griffiths, and D. Vella, Physical Review Fluids **2**, 014202 (2017).

[14] O. Oshri, Y. Liu, J. Aizenberg, and A. C. Balazs, Physical Review E **97**, 062803 (2018).

[15] L. Boué, M. Adda-Bedia, A. Boudaoud, D. Cassani, Y. Couder, A. Eddi, and M. Trejo, Physical Review Letters **97**, 166104 (2006).

[16] M. Adda-Bedia, A. Boudaoud, L. Boué, and S. Deboeuf, Journal of Statistical Mechanics: Theory and Experiment **2010**, P11027 (2010).

[17] C. Donato and M. Gomes, Physical Review E **75**, 066113 (2007).

[18] N. Stoop, J. Najafi, F. K. Wittel, M. Habibi, and H. Herrmann, Physical Review Letters **106**, 214102 (2011).

[19] R. Vetter, F. K. Wittel, and H. J. Herrmann, Nature Communications **5**, 1 (2014).

[20] B. Florijn, C. Coulais, and M. van Hecke, Physical Review Letters **113**, 175503 (2014).

[21] J. Paulose, A. S. Meeussen, and V. Vitelli, Proceedings of the National Academy of Sciences **112**, 7639 (2015).

[22] T. Frenzel, C. Findeisen, M. Kadic, P. Gumbsch, and M. Wegener, Advanced Materials **28**, 5865 (2016).

[23] K. Bertoldi, V. Vitelli, J. Christensen, and M. Van Hecke, Nature Reviews Materials **2**, 1 (2017).

[24] B. McCoy and T. Wu, *The Two-Dimensional Ising Model: Second Edition* (Dover Publications, 2014), ISBN 9780486783123, URL `https://books.google.com/books?id=YO4xAwAAQBAJ`.

[25] R. P. Feynman, *Statistical mechanics: a set of lectures* (CRC press, 2018).

[26] S. H. Kang, S. Shan, A. Košmrlj, W. L. Noorduin, S. Shian, J. C. Weaver, D. R. Clarke, and K. Bertoldi, Physical Review Letters **112**, 098701 (2014).

[27] M. E. H. Bahri, S. Sarkar, and A. Košmrlj, arXiv preprint arXiv:2209.09350 (2022).

[28] P. Z. Hanakata, A. Plummer, and D. R. Nelson, Physical Review Letters **128**, 075902 (2022).

[29] D. Nelson, T. Piran, and S. Weinberg, *Statistical mechanics of membranes and surfaces* (World Scientific, 2004).

[30] A. P. Thompson, H. M. Aktulga, R. Berger, D. S. Bolintineanu, W. M. Brown, P. S. Crozier, P. J. in't Veld, A. Kohlmeyer, S. G. Moore, T. D. Nguyen, et al., Computer Physics Communications **271**, 108171 (2022).

[31] A. Stukowski, Modelling and Simulation in Materials Science and Engineering **18**, 015012 (2009).

[32] A. Guerra and D. P. Holmes, Soft Matter **17**, 7662 (2021).

[33] J.-F. Sadoc and R. Mosseri, *Geometrical frustration* (1999).

[34] N. Weiner, Y. Bhosale, M. Gazzola, and H. King, Journal of Applied Physics **127**, 050902 (2020).

[35] W. van Adrichem and K. Newman, Journal of Petroleum Technology **45**, 155 (1993).

[36] G. Gao and S. Z. Miska, SPE Journal **14**, 782 (2009).

[37] J. T. Miller, C. G. Mulcahy, J. Pabon, N. Wicks, and P. M. Reis, Journal of Applied Mechanics **82** (2015).

[38] S. Poincloux, T. Chen, B. Audoly, and P. M. Reis, Physical Review Letters **126**, 218004 (2021).

[39] T. Elder, T. Twohig, H. Singh, and A. B. Croll, Soft Matter **16**, 10611 (2020).

[40] A. B. Croll, Y. Liao, Z. Li, W. M. Jayawardana, T. Elder, and W. Xia, Matter (2022).

[41] D. J. Needleman, M. A. Ojeda-Lopez, U. Raviv, K. Ewert, J. B. Jones, H. P. Miller, L. Wilson, and C. R. Safinya, Physical review letters **93**, 198104 (2004).

[42] E. Joselevich, H. Dai, J. Liu, K. Hata, and A. H Windle, Carbon nanotubes pp. 101–165 (2007).

[43] E. G. Rakov, Russian Chemical Reviews **82**, 538 (2013).

[44] L. Wu, Y. Wang, Z. Zhai, Y. Yang, D. Krishnaraju, J. Lu, F. Wu, Q. Wang, and H. Jiang, Applied Materials Today **20**, 100671 (2020).

[45] P. Packo, A. N. Norris, and D. Torrent, Physical Review Applied **15**, 014051 (2021).